Mechanical behavior and microstructure properties of titanium powder consolidated by high-pressure torsion

Alexander P. Zhilyaev, Geoffrey Ringot, Yi Huang, Jose Maria Cabrera, Terence G. Langdon

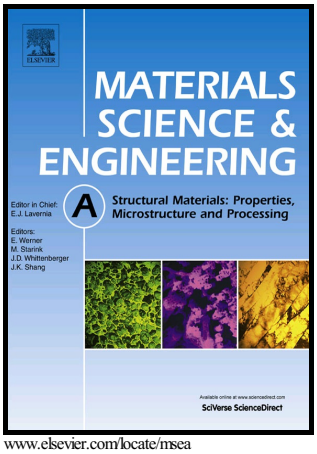

www.elsevier.com/locate/msea

PII: S0921-5093(17)30189-2
DOI: http://dx.doi.org/10.1016/j.msea.2017.02.032
Reference: MSA34708

To appear in: *Materials Science & Engineering A*

Cite this article as: Alexander P. Zhilyaev, Geoffrey Ringot, Yi Huang, Jose Maria Cabrera and Terence G. Langdon, Mechanical behavior and microstructure properties of titanium powder consolidated by high-pressure torsion, *Material Science & Engineering A,* http://dx.doi.org/10.1016/j.msea.2017.02.032

Mechanical behavior and microstructure properties of titanium powder consolidated by high-pressure torsion

Alexander P. Zhilyaev[1,2,3], Geoffrey Ringot[4], Yi Huang[5], Jose Maria Cabrera[6], Terence G. Langdon[5,7*]

[1]Institute for Metals Superplasticity Problems, Khalturina 39, Ufa, 450001, Russia
[2]Fundació CTM Centre Tecnològic, Plaça de la Ciencia 2, Manresa, Barcelona, 08242, Spain
[3]Research Laboratory for Mechanics of New Nanomaterials, Peter the Great St. Petersburg Polytechnic University, Polytechnicheskaya 29 St. Petersburg, 195251, Russia
[4]École Nationale Supérieure des Ingénieurs en Arts Chimiques et Technologiques (ENSIACET), National Polytechnic Institute of Toulouse (INPT), 31077 Toulouse CEDEX 04, France
[5]Materials Research Group, Faculty of Engineering and the Environment, University of Southampton, Southampton SO17 1BJ, UK
[6]Departamento de Ciencia de los Materiales e Ingeniería Metalúrgica, ETSEIB – Universitat Politècnica de Catalunya, Av. Diagonal 647, Bacelona, 08028, Spain
[7]Departments of Aerospace & Mechanical Engineering and Materials Science, University of Southern California, Los Angeles, CA 90089-1453, USA
*Corresponding author: Terence G. Langdon: langdon@usc.edu

Abstract.

Research was conducted to investigate the potential for consolidating titanium powder using high-pressure torsion (HPT) at room temperature. The nanostructured samples processed by HPT were characterized by X-ray diffraction (XRD) and transmission electron microscopy (TEM). The results show there is a significant refinement of the Ti powder and it consolidates into bulk nanostructured titanium with a mean grain size estimated by TEM as ~200-300 nm and a mean crystallite size measured by XRD as ~20-30 nm. Microhardness measurements and tensile testing show high strength and low ductility after consolidation under a pressure of 6.0 GPa for 5 revolutions. Additional short annealing at a temperature of 300°C for 10 minutes leads to a significant enhancement in ductility while maintaining the high strength.

Keywords: high-pressure torsion, mechanical properties, microstructure, titanium powder

1. Introduction

Processing bulk nanostructured materials [1] through the application of severe plastic deformation (SPD) [2], using techniques such as equal-channel angular pressing (ECAP) [3] and high-pressure torsion (HPT) [4], is now recognized as an important tool for achieving grain refinement. However, less attention has been paid to the very powerful ability of HPT to consolidate metallic powders [5, 6, 7, 8. 9], as well as composites [10, 11, 12, 13, 14], amorphous compounds [15, 16, 17, 18. 19], machining chips [20, 21, 22] and even ceramic powders [23].

Titanium and titanium alloys are excellent metals for structural and bioengineering applications due to their high corrosion resistance and biocompatibility [24, 25, 26, 27, 28]. Since pure Ti has low strength, alloying with other elements is generally used to increase its mechanical strength but this may lead to degradation in biocompatibility. To solve this problem, processing by SPD may be used to improve the mechanical properties of pure titanium. One way deserving special attention is to produce bulk nanostructured titanium through the cold consolidation of titanium powder by means of HPT. In order to significantly increase the strength, there is a report of ball-milled (BM) powder of Ti which was consolidated by HPT to form bulk nanocrystalline disks [29]. A relative high density (99.9%) and a high tensile strength were achieved after cold consolidation from ball-milled titanium powder and an additional sample was also consolidated from a non-BM Ti powder. Although the published information is limited, it appears from the report that this specimen exhibited not only a high strength but also a reasonable level of ductility. Based on these results, research was initiated specifically to examine the mechanical properties and the microstructural evolution of HPT-consolidated titanium powder.

2. Experimental materials and procedures

Experiments were conducted on commercial purity (CP) titanium powder (99.5 wt.%) having a mesh size of ~150 μm obtained from Goodfellow Ltd., Cambridge, UK. The chemical composition of the Ti powder was (in ppm) C < 100, chlorides 1700, Fe 200, N <100, O 1000. The powder was pre-compacted into disk-shaped tablets with diameters of 10 mm and thicknesses of approximately 1.5 mm. These tablets were further consolidated to thicknesses of ~0.85 mm by HPT under an applied pressure of 6.0 GPa for 1 minute without any anvil rotation so that no torsional deformation was applied. These consolidated powder Ti samples are henceforth designated N0 samples. Some N0 samples were selected for annealing in an argon atmosphere at 700°C for 40 min and they were used as a reference to show the initial coarse-grained material of powder Ti before HPT processing. Figure 1 shows an optical image of the microstructure of the Ti powder specimen processed by simple compression and then annealed at 700°C for 40 min. The mean grain size was measured by the intercept method using ImageJ™ [30] and this gave 85.1 ± 29.5 μm. The remaining N0 samples were then further processed by HPT at room temperature (RT) under an applied pressure, *P*, of 6.0 GPa, using a rotation speed of 1 rpm and torsional straining through numbers of revolutions, *N*, of 5 turns and then annealed for 10 min in air at consecutive temperatures of 250, 300, 450, 650 and 750°C.

All disks were polished to a mirror-like quality and hardness measurements were taken using a Vickers micro-hardness tester with a load of 500 gf and a dwell time of 10 s. The average microhardness values, Hv, were measured along randomly selected diameters on each disk. These measurements were taken at intervals of 0.5 mm and at every point the local value of Hv was obtained from the average of four separate hardness values.

The analyses by X-ray diffraction (XRD) were undertaken using a Bruker D2 Phaser instrument with Cu radiation ($K_{\alpha 1}$ = 1.54060 Å) and a Ni monochromator with a 1D LYNXEYE detector. The scan step was 0.02° and the delay time was 2.5 s. A Rietveld analysis using MAUD

software [31] was performed in order to monitor the phase composition, the lattice parameters, *a*, c, the microcrystallite size, *d*, and the microstrain $<\varepsilon^2>^{1/2}$.

Transmission electron microscopy (TEM) (JEOL) was employed to characterize the fine microstructure of nanostructured titanium after processing by HPT. Foils for TEM studies were cut out by electro-discharge machining (EDM). After mechanical thinning to about 100 µm, they were subjected to electrolytic polishing using a "Tenupol-5" set. Electropolishing was conducted using chemical solution consisting of 5% perchloric acid, 35% butanol and 60% methanol in the temperature range of −20 to -35 °C. The grain size distribution was obtained by examining at least 5 dark field images for each sample. Since many low-angle boundaries were not well-defined in this analysis and hence these boundaries were discounted, the grains used for detailed analysis are primarily those separated by high-angle misorientations. The mean grain size was defined as the diameter of a circle with the same area as a grain in the dark field image, so that $d=(4\cdot S/\pi)^{1/2}$. The area of the individual grains was measured using the ImageJ software.

For mechanical testing, two miniature tensile specimens were cut from symmetric off-centre positions in each disk near the edges using EDM. This specimen configuration was described earlier and the gauge dimensions were 1.1 x 1.0 x 0.6 mm^3 [32].

The mechanical properties were examined at room temperature and at elevated temperatures of 250 and 300°C. All specimens were heated rapidly to the testing temperature, typically in a time of ~5–10 min, and then held for 10 min to reach a uniform temperature prior to testing. Stress-strain curves were recorded using an initial strain rate of 1.0 x 10^{-3} s^{-1}. The stress-strain curves were plotted for each specimen and the yield stress (YS) and the ultimate tensile strength (UTS) were then measured from each curve. At least two samples were tested for each condition. All elongations were carefully calculated by measuring the gauge lengths before and after tensile testing using an optical microscope.

3. Experimental results

3.1 Microhardness

Figure 2 shows results for the microhardness measurements. The microhardness distribution along the diameter of the HPT-processed Ti powder compressed to a disk is given in Fig. 2a. It is apparent that after pure compression without torsional straining (P = 6.0 GPa, N = 0 and loading time of 1 min) and annealing at 700°C for 40 min the microhardness distribution is highly inhomogeneous along the disk diameter. This inhomogeneity is so large that there is a difference in Hv of up to more than 100%. By contrast, after HPT processing for 5 whole revolutions the microhardness is essentially fully homogeneous and equal to Hv ≈ 300. This latter value is consistent with earlier results [27] where the microhardness for consolidated BM titanium powder was Hv ≈ 350. Figure 2b shows the evolution in the disk consolidated for 5 whole revolutions and annealed for 10 minutes at consecutive temperatures of 250, 300, 450, 650 and 700 °C. This plot shows that the HPT-consolidated Ti powder is thermostable in short annealing but there is a drop of about 50 Hv in the microhardness value between 450 and 650 °C.

3.2 XRD results

The crystallite size and microstrain were measured by XRD using Rietveld refinement in the MAUD software. Figure 3 shows a typical example of the analysis for an HPT-consolidated disk at P = 6.0 GPa and N = 5 turns. Thus, the material is single alpha-phase titanium and neither the omega phase nor titanium oxides were detected or if these phases exist then they are below the detectable level of the XRD analysis. This is not consistent with the earlier result using BM Ti powder [27] where an omega phase was detected in a sample consolidated at P = 6.0 GPa through 4 whole revolutions. As noted earlier [33], the alpha-omega phase transformation represents the accommodation process during HPT processing of metals of Group VI of the periodic table. Obviously in the nanocrystalline BM Ti powder used earlier[27] the grain size

was already in the nanometer range so that any dislocation movement was difficult. By contrast, in the present investigation using Ti powder with large particles (~150 μm mesh), dislocation slip was an active deformation process.

The XRD results on the evolution of the crystallite size and the microstrain of the samples of HPT-consolidated Ti powder are shown in Fig.4a, where HPT_0 is assigned for the sample compressed without torsion (HPT, *P* = 6.0 GPa. *N* = 0, loading for 1 min) and annealed at 700°C for 40 min and HPT_5 corresponds to the disk of Ti powder consolidated at room temperature for 5 whole revolutions at a load of 6.0 GPa. The microstrain was obtained from the MAUD software which is a full profile analysis based on full-width at half-maximum (FWHM). The additional datum points for HPT+250 and HPT+300 in Fig. 4a correspond to the disks processed at a load of 6.0 GPa for 5 whole revolutions and additionally annealed for 10 min at 250 and 300°C. Thus, the crystallite size decreases more than 3 times during HPT consolidation at room temperature and then slightly increases during the subsequent short annealing. Evidently, the microstrain has a reciprocal trend increasing to a maximum for HPT-consolidated disks of titanium and decreasing during annealing. It is worth noting that during the short annealing at 250°C the microstrain decreases more than 2 times whereas the crystallite size increases only by ~20% from 36.9 nm to 42.4 nm. During annealing at 300°C the microstrain decreases slightly but there is a continuously increasing crystallite size. Apparently at the lower temperature (250°C) there is mostly a relaxation of the microstrain whereas at higher temperatures (300°C) some growth of the crystallites (subgrains) can occur.

Figure 4b shows the dislocation density evolution calculated from the XRD results using the equation [34, 35]:

$$\rho = \frac{2\sqrt{3}\cdot\langle\varepsilon^2\rangle^{1/2}}{d\cdot a}, \qquad (1)$$

where $\langle \varepsilon^2 \rangle^{1/2}$ is the microstrain, d is the crystallite size and a = 2.95 Å is the Burgers vector for ‹a›-type of dislocations in alpha titanium. It is known that with increasing of accumulated strain ‹a›- and ‹$c+a$›- types of dislocations prevail in the microstructure of alpha titanium [36]. Thus, equation (1) may overestimate the dislocation density but nevertheless it was used to provide a relative comparison. The dislocation density has the same trend as the microstrain, achieving a very high level of 6.6×10^{14} m^{-2} which is a typical level for HPT-processed metals and alloys [4]. After a short annealing, it is apparent that the dislocation density decreases more than 3 times.

3.3 TEM results

The fine microstructure of the Ti-consolidated powder after HPT processing and short term annealing is shown in Fig. 5. The typical HPT structure for the disk processed at room temperature (Fig. 5a) consists of grains of ~100 nm with blurred grain boundaries and typical selected area diffraction patterns (SAED) showing rings of diffraction spots. The dark field image in Fig. 5b reveals grains of different sizes. Figures 5c and 5d represent bright and dark field images of the specimen annealed at 250°C for 10 min. Thus, the grain size does not increase significantly but the grain boundaries become more sharp and well-defined. The SAED pattern consists of fairly discontinuous spots showing microstrain relief. Thus, these data support the findings from the XRD. Figures 5 e and f show the microstructure of the HPT-consolidated titanium annealed at 300°C for 10 min but with a different scale bar compared with the other images. Thus, grains with very sharp boundaries with a size of ~ 200 nm appear in the structure suggesting that the microstructure recovers and the (sub-)grains grow. Using more than 10 dark field images for each condition, the grain size was estimated by measuring the area of the grains and calculating a diameter of the circle with equivalent area using the relationship:

$$d = \sqrt{4 \cdot S/\pi}, \qquad (2)$$

where d is the grain size and S is the area of grains in the dark field (DF) images.

Figure 6 depicts the corresponding grain size distributions. The mean grain size, *d*m, was calculated as *d*m ≈ 202.5 ± 71.9 nm for the HPT-consolidated disk of powder titanium, 213.9 ± 63.6 nm for the sample annealed at 250°C and 237.0 ± 69.1 nm for the disk annealed at 300°C. Due to the relatively small statistics, these results have a high dispersion. Nevertheless, a trend of increasing grain size is evident. In Fig. 6, all data were approximated by Gaussian distributions with coordinates for the centre of 193.5, 198.0 and 228.6 nm for the HPT samples and after annealing at 250°C and 300°C, respectively. These values correspond to the trend observed from the XRD results, with minimal (sub)-grain growth at the lower annealing temperature (250°C) and noticeable growth at the higher annealing temperature (300°C).

3.4 Tensile testing

Representative plots of engineering stress against engineering strain are shown in Fig. 7 for the HPT- consolidated titanium powder. It is interesting to note that all specimens, except only the sample annealed at 300°C for 10 min, show zero ductility and fail essentially within the elastic region.

4. Discussion

4.1 Microhardness

The low microhardness and pronounced inhomogeneity of the compacted Ti powder is related to the lack of full densification of the sample under compression without straining. Fully annealed Grade 2 titanium has a microhardness value of ~170 [32] and this value correlates well with the microhardness in the edge region of the compacted disk. Therefore, it is concluded that the radial shear deformation present during pure compression of the disk assists directly in the densification of the titanium powder. Using the Archimedes method for measuring density gave a range of densities between 0.90 and 0.95 of the value for the bulk Ti density where the high scatter is due to the small mass of the HPT disk (< 0.5 mg). It should be

noted that HPT processing at *P* = 6.0 GPa for 5 whole revolution gives the same level of microhardness (~300 Hv) as for bulk Ti [32].

4.2 XRD and TEM data

In bulk titanium the increase in microhardness and consequently enhanced strength is generally related to the presence of an ω-phase in the α-matrix of titanium. However, for powder titanium subjected to HPT (P = 6.0 GPa, N = 5, RT) the ω-phase was not detected from the X-ray analysis in Fig. 3. The absence of the ω-phase can be rationalized in two ways. First, impurities such as a high oxygen content can block the α→ω transformation [37]. Second, it may be due to the granular nature of the sample so that the internal strain failed to reach a level sufficient for stabilizing the ω-phase and instead a reverse transformation occurred after releasing the pressure. The TEM micrographs in Fig. 5 a and b support the absence of the ω-phase because the SAED has no rings corresponding to this phase.

The grain size distributions obtained from the TEM dark field micrographs suggest a Gaussian-type for the specimens after annealing at 250 and 300 °C for 10 min. However, for the HPT-processed disk the grain size distribution appears bimodal with separate peaks at ~125 nm and at ~225 nm.

4.3 Mechanical behavior

An evaluation of the Young´s modulus was made only from the stress-strain plot and therefore the value is not precise. However, careful inspection showed a trend that the compressed sample (HPT, *P* = 6.0 GPa, *N* = 0, loading for 1 min) and annealed at 700°C for 40 min showed an elongation of about 0.006 and it gave a slope of 88.9 GPa which is significantly lower than the value of Young's modulus for coarse-grained alpha titanium of ~110.3 GPa. This difference is attributed to the retained porous structure of the compressed powder titanium. The HPT-consolidated Ti powder processed by torsional straining to 5 revolutions showed a slope of ~136.8 GPa which is higher than for the coarse-grained material but is consistent with

experimental observations showing that SPD leads in general to an increase in the Young's modulus [38]. The increasing Young's modulus for nanostructured materials is related to the high internal stresses induced directly by these processing methods. Conversely, annealing at 250°C brings the Young's modulus back to the level of coarse-grained titanium at 117.2 GPa. This value of Young modulus was estimated for the sample annealed at 300°C.

All specimens showed little ductility except for the sample annealed at 300 °C for 10 min. It is apparent from Fig. 7 that this specimen showed enhanced plasticity of ~2.2%. In practice, this is lower than the plasticity of ~8% reported for the consolidated BM powder subjected to 10 whole revolutions [29]. It is worth noting that apparently during HPT straining to 10 revolutions the titanium underwent a reverse omega to alpha phase transformation which can increase the final ductility.

In the present investigation, there was no evidence for any omega phase and this means that the origin of the high tensile stress is due to another effect. It seems probable that a small titanium oxide layer was broken into particles by HPT giving an average size, D_P, of ~2 nm which is the typical oxide layer for titanium. Then for these randomly distributed particles, the centre-to-centre nearest neighbour spacing on a plane may be calculated from the relationship [39]:

$$L_P = \frac{D_P}{2}\sqrt{\frac{\pi}{6F_V}} \qquad (3)$$

where F_V = 4 x 10^{-5} is the volume fraction of titanium oxide in the titanium matrix. A straightforward estimation gives ~114.4 nm. Applying the conventional Baker-Kocks-Scattergood (BKS) modification of the Orowan model [40]:

$$\sigma_{BKS} = A\frac{MGb}{L_P}\left[ln\left(\frac{D_P}{2b}\right) + 0.7\right] \qquad (4)$$

where the BKS stress is estimated as ~129.6 MPa. This is necessarily a rough estimate because, in the absence of detailed high-resolution TEM, the particle size and distribution are not known.

Nevertheless, it is apparent that the estimate gives a very reasonable value for the particle hardening.

5. Summary and conclusions

A study of CP titanium powder processed by HPT revealed that:

1. Bulk dense disks of titanium powder were consolidated by applying HPT at a load of 6.0 GPa through 5 whole revolutions.
2. The consolidated samples had an ultrafine grain size, a nanometer crystallite size, a very high level of internal stress and a correspondingly high dislocation density. As a result, their behavior was generally brittle in tensile testing.
3. Short annealing for 10 minutes at 250°C led to a relaxation of the internal stress and no significant (sub)-grain growth. Annealing at the higher temperature of 300°C led to a significantly increased ductility up to ~2.2 %.

Conflict of Interest:

The authors declare that they have no conflict of interest.

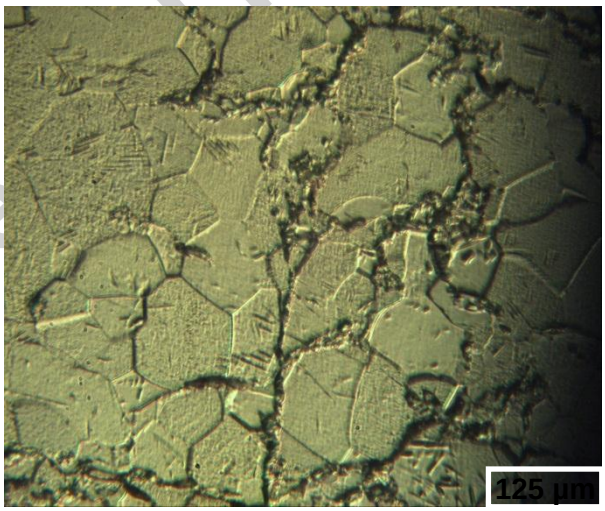

Fig. 1. Optical image of HPT consolidated titanium powder (P = 6.0 GPa, N = 0, loading time = 1 min + annealing at 700°C for 40 min) (d = 85.1 ± 29.5 µm).

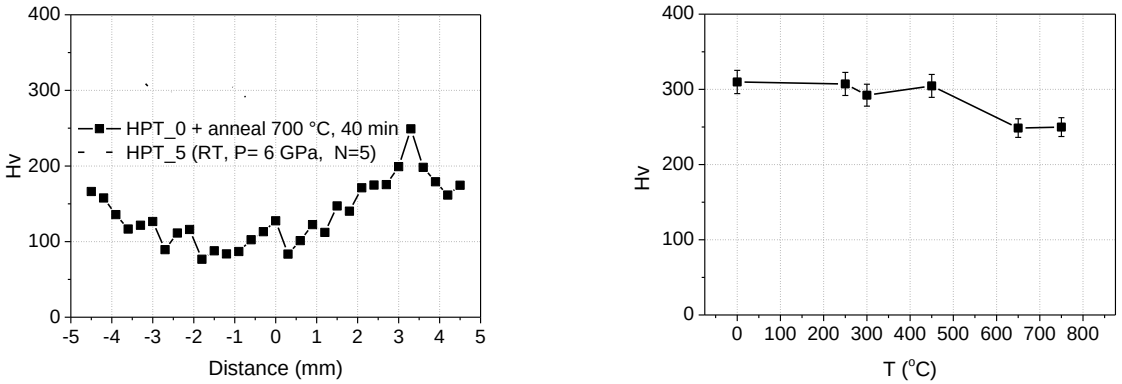

a) b)

Fig. 2. Microhardness, Hv (a) across the disk diameter and (b) as a function of annealing temperature for HPT consolidated Ti powder.

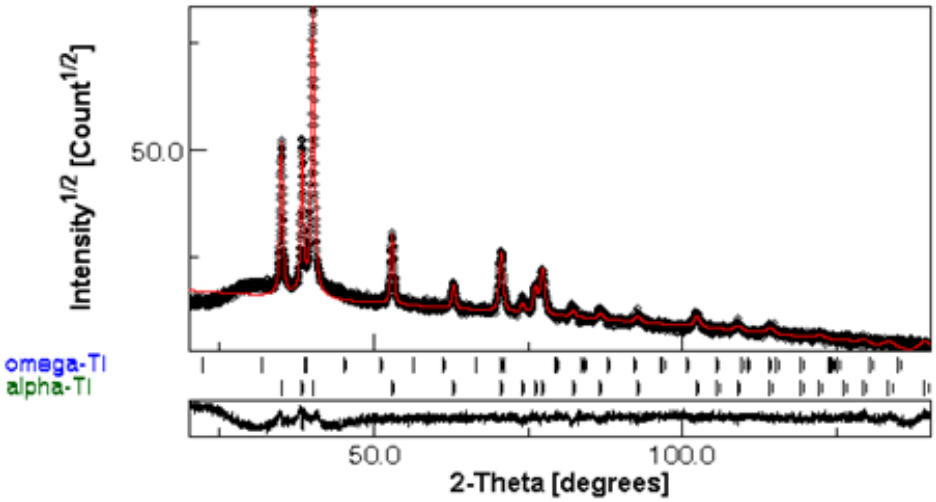

Fig.3. An example of Rietveld analysis of HPT consolidated titanium powder (RT, P = 6.0 GPa, N = 5) by MAUD software: red line is a calculated fitting curve.

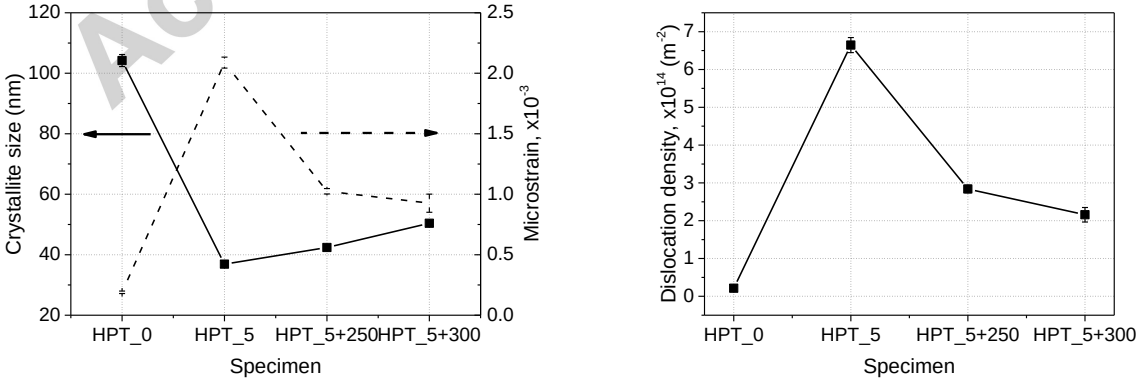

Fig. 4. (a) Crystallite size and microstrain and (b) dislocation density as a function of the sample conditions (HPT_0 corresponds to the compression at P = 6.0 GPa, N = 0, loading for 1 min; HPT_5 corresponds to HPT straining of Ti powder at P = 6.0 GPa, N = 5; HPT+250 and HPT+300 are HPT specimens with annealing for 10 min at 250 and 300°C, respectively.

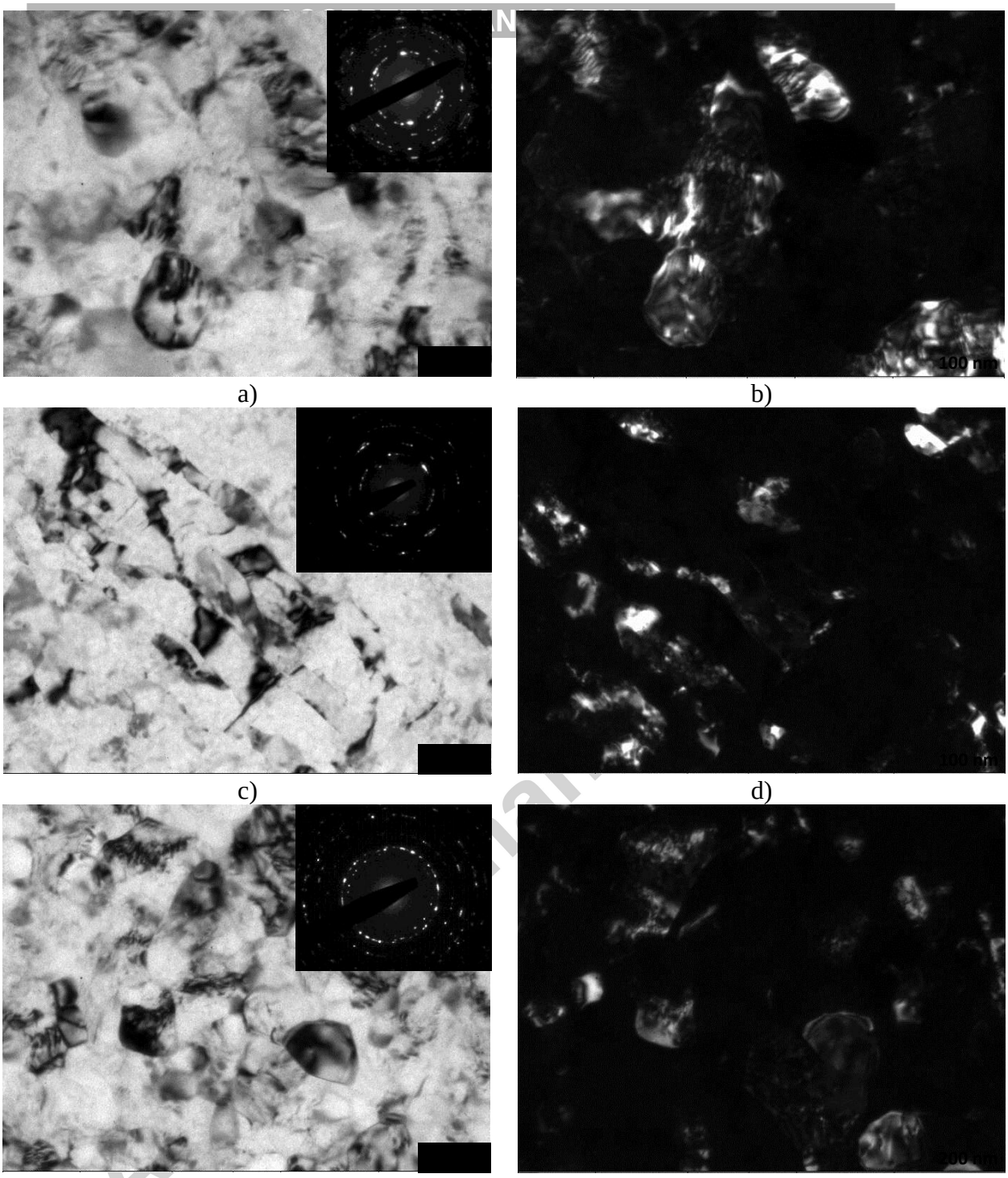

Fig. 5. Bright (a, c, e) and dark (b, d, f) field TEM of Ti powder consolidated by HPT (P = 6.0 GPa and N = 5) (a, b) and annealed at 250°C for 10 min (c, d) and annealed at 300°C for 10 min (e, f). Inset depicts SAED.

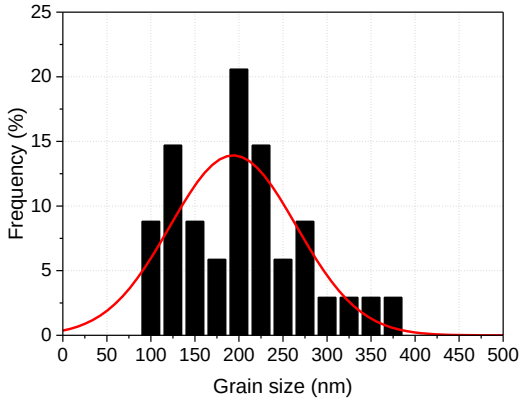

a)

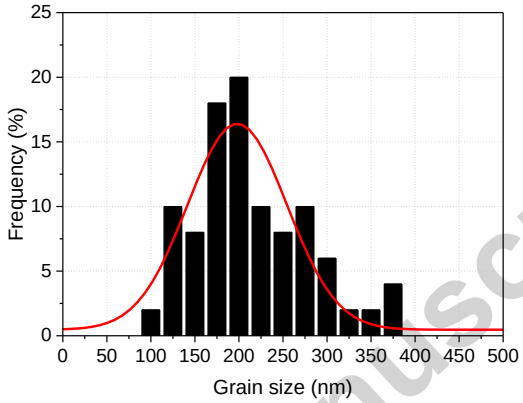

b)

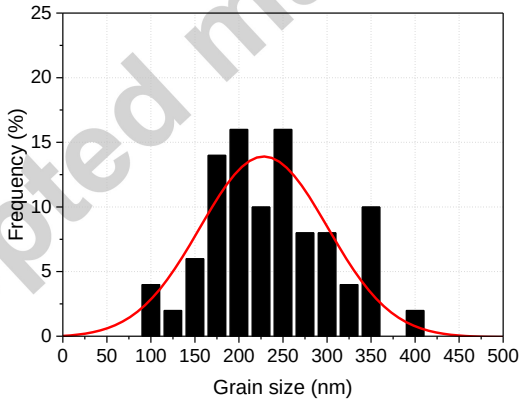

c)

Fig. 6. Grain size distribution for the Ti powder consolidated by HPT (P = 6.0 GPa and N = 5) (a) and annealed at 250°C for 10 min (b) and annealed at 300°C for 10 min (c).

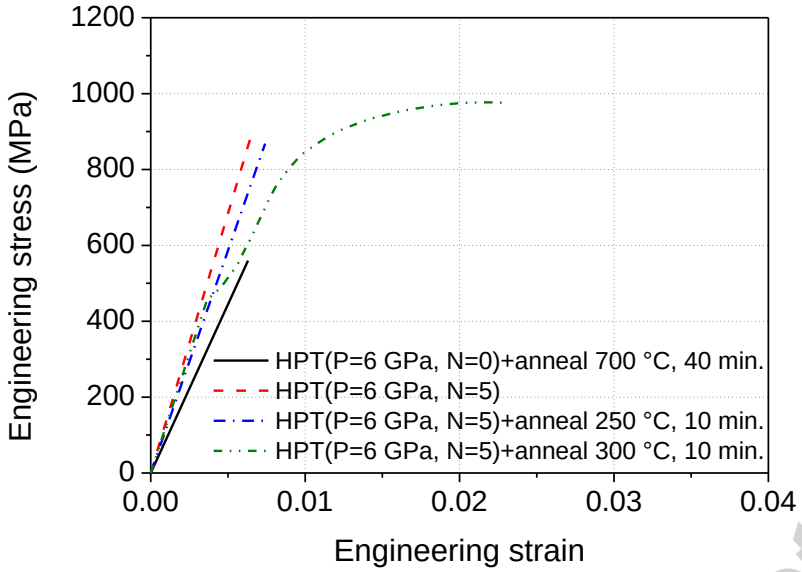

Fig. 7. Engineering stress/strain plots for powder Ti subjected to HPT (RT, P = 6.0 GPa, N = 5) and additional annealing for 10 min at T = 250 and T = 300°C. Black dot line is tensile plot for the samples annealed at 700°C for 40 min. All annealing were performed in vacuum (10^{-3} torr.), strain rate was 10^{-3} s^{-1}.

Acknowledgments

APZ acknowledges a TECNIOSPRING grant financed by Generalitat de Catalunya and co-funded by the 7th Framework program of the EU and the Russian Science Foundation (Project 14-29-00199). YH and TGL acknowledge support from the European Research Council under ERC Grant Agreement No. 267464-SPDMETALS.

References

[1] R.Z. Valiev, I.V. Alexandrov, Y.T. Zhu, T.C. Lowe. Paradox of strength and ductility in metals processed by severe plastic deformation. J. Mater. Res. 17(2002) 5–8.

[2] R.Z. Valiev, A.P. Zhilyaev, T.G. Langdon. Bulk nanostructured materials: Fundamentals and applications. Wiley, Hoboken, NJ, USA, 2014, 450p.

[3] R.Z. Valiev, T.G. Langdon. Principles of equal-channel angular pressing as a processing tool for grain refinement. Prog. Mater. Sci. 51 (2006) 881–981.

[4] A.P. Zhilyaev, T.G. Langdon. Using high-pressure torsion for metal processing: Fundamentals and applications. Prog. Mater. Sci. 53 (2008) 893–979.

[5] A.V. Korznikov, I.M. Safarov, D.V. Laptionok, R.Z. Valiev. Structure and properties of superfine-grained iron compacted out of ultradisperse powder. Acta. Metall. Mater. 39 (1991) 3193-3197.

[6] H. Shen, B. Guenther, A.V. Korznikov, R.Z. Valiev. Influence of powder consolidation methods on the structural and thermal properties of a nanophase Cu-50wt%Ag alloy. Nanostruct. Mater. 6 (1995) 385-388.

[7] R.Z. Valiev, R.S. Mishra, J. Groza, A.K. Mukherjee. Processing of nanostructured nickel by severe plastic deformation consolidation of ball-milled powder. Scripta Mater. 34 (1996) 1443-1448.

[8] J. Sort, A.P. Zhilyaev, M. Zielinska, J. Nogues, S. Surinach, J. Thibault , M.D. Baro. Microstructural effects and large microhardness in cobalt processed by high pressure torsion consolidation of ball milled powders. Acta Mater. 51 (2003) 6385-6393.

[9] Z. Lee, F. Zhou, R.Z. Valiev, E.J. Lavernia, S.R. Nutt. Microstructure and microhardness of cryomilled bulk nanocrystalline Al-7.5%Mg alloy consolidated by high pressure torsion. Scripta Mater. 51 (2004) 209-214.

[10] E. Menendez, J. Sort, V. Langlais, A. Zhilyaev, J.S. Munoz, S. Surinach, J. Nogues, M.D. Baro. Cold compaction of metal–ceramic (ferromagnetic–antiferromagnetic) composites using high pressure torsion. J. Alloys. Comp. 434-435 (2007) 505-508.

[11] E. Menendez, G. Salazar-Alvarez, A.P. Zhilyaev, S. Surinach, M.D. Baro, J. Nogues, J. Sort. Cold consolidation of metal-ceramic nanocomposite powders with large ceramic fractions. Adv. Funct. Mater. 18 (2008) 3293-3298.

[12] H. Li, A. Misra, Y. Zhu, Z. Horita, C.C. Koch, T.G. Holesinger. Processing and characterization of nanostructured Cu-carbon nanotube composites. Mater. Sci. Eng. A 523 (2009) 60-64.

[13] H. Li, A. Misra, Z. Horita, C.C. Koch, N.A. Mara, P.O. Dickerson, Y. Zhu. Strong and ductile nanostructured Cu-carbon nanotube composite. J. Appl. Phys. 95 (2009) 071907(1-4).

[14] A. Bachmaier, A. Hohenwarter, R. Pippan. New procedure to generate stable nanocrystallites by severe plastic deformation. Scripta Mater. 61 (2009) 1016-1619.

[15] J. Sort, D.C. Ile, A.P. Zhilyaev, A. Concustell, T. Czeppe, M. Stoica, S. Surinach, J. Eckert, M.D. Baro. Cold-consolidation of ball-milled Fe-based amorphous ribbons by high pressure torsion. Scripta Mater. 50 (2004) 1221-1225.

[16] A.R. Yavari, W.J. Botta, C.A.D. Rodrigues, C. Cardoso, R.Z. Valiev. Nanostructured bulk $Al_{90}Fe_5Nd_5$ prepared by cold consolidation of gas atomised powder using severe plastic deformation. Scripta Mater. 46 (2002) 711-716.

[17] Z. Kovacs, P. Henits, A.P. Zhilyaev, A. Revesz. Deformation induced primary crystallization in a thermally non-primary crystallizing amorphous $Al_{85}Ce_8Ni_5Co_2$ alloy. Scripta Mater. 54 (2006) 1733-1737.

[18] N. Boucharat, R. Hebert, H. Rosner, R.Z. Valiev, G. Wilde. Synthesis routes for controlling the microstructure in nanostructured $Al_{88}Y_7Fe_5$ alloys. J. Alloys. Comp. 434-435 (2007) 252-254.

[19] T. Czeppe, G. Korznikova, J. Morgiel, A. Korznikov, N.Q. Chinh, P. Ochin, A. Sypien. Microstructure and properties of cold consolidated amorphous ribbons from (NiCu)ZrTiAlSi alloys. J. Alloys Comp. 483 (2009) 74-77.

[20] A.P. Zhilyaev, A.A. Gimazov, G.I. Raab, T.G. Langdon. Using high-pressure torsion for the cold-consolidation of copper chips produced by machining. Mater Sci Eng A 486 (2008) 123-128.

[21] A.P. Zhilyaev, S. Swaminathan, A.A. Gimazov, T.R. McNelley, T.G. Langdon. An evaluation of microstructure and microhardness in copper subjected to ultra-high strains. J. Mater. Sci. 43 (2008) 7451-7456.

[22] K. Edalati, Y. Yokoyama, Z. Horita. High-pressure torsion of machining chips and bulk discs of amorphous $Zr_{50}Cu_{30}Al_{10}Ni_{10}$. Mater. Trans. 51 (2010) 23-26.

[23] K. Edalati, Z. Horita. Application of high-pressure torsion for consolidation of ceramic powders. Scripta Mater. 63 (2010) 174-177.

[24] C. Leyens, M. Peters. Titanium and Titanium Alloys Fundamentals and Applications, Wiley, Darmstadt, Germany, 2003.

[25] C.N. Elias, J.H.C. Lima, R. Valiev, M.A. Meyers. Biomedical applications of titanium and its alloys. JOM 60 (2008) 46-49.

[26] R.Z. Valiev, I. Sabirov, A.P. Zhilyaev, T.G. Langdon. Bulk nanostructured metals for innovative applications. JOM 64 (2012) 1134-1142.

[27] C.T. Wang, A.G. Fox, T.G. Langdon. Microstructural evolution in ultrafine-grained titanium processed by high-pressure torsion under different pressures. J. Mater. Sci. 49 (2014) 6558-6564.

[28} Y.J. Chen, Y.J. Li, J.C. Walmsley, N. Gao, H.J. Roven, M.J. Starink, T.G. Langdon. Microstructural heterogeneity in hexagonal close-packed pure Ti processed by high-pressure torsion. J. Mater. Sci. 47 (2012) 4838-4844.

[29] K. Edalati, Z. Horita, H. Fujiwara, K. Ameyama. Cold Consolidation of Ball-Milled Titanium Powders Using High-Pressure Torsion. Metal. Mater. Trans. A 41 (2010) 3308-3317.

[30] ⟨https://imagej.nih.gov/ij/⟩ (ImageJ free software).

[31] ⟨http://maud.radiographema.com/⟩ (MAUD free software).

[32] H. Shahmir, P.H.R. Pereira, Y. Huang, T.G. Langdon. Mechanical properties and microstructural evolution of nanocrystalline titanium at elevated temperatures. Mater. Sci. Eng. A 669 (2016) 358-366.

[33] M.T. Perez-Prado, A.P. Zhilyaev. First Experimental Observation of Shear Induced hcp to bcc Transformation in Pure Zr. Phys. Rev. Let. 102 (2009) 175504(1-4).

[34] G.K. Williamson, R.E. Smallman. III. Dislocation densities in some annealed and cold-worked metals from measurements on the X-ray debye-scherrer spectrum. Philos. Mag. 1 (1956) 34-46.

[35] R.E. Smallman, K.H. Westmacott. Stacking faults in face-centered cubic metals and alloys. Philos. Mag. 2 (1957) 669-683.

[36] I.C. Dragomir, G A. Castello-Branco, G. Ribarik, H. Garmestani, T. Ungar, R. L. Snyder. Burgers vector populations in hot rolled titanium determined by X-ray peak profile analysis. Zeitschrift fur Kristallographie, Supplement 1(23) (2006) 99-104.

[37] R.G. Hennig, D.R. Trinkle, J. Bouchet, S.G. Srinivasan, R.C. Albers, J.W. Wilkins, Impurities block the α to ω martensitic transformation in titanium. Nature Mater. 4 (2005) 129-133.

[38] G. Wang, X. Li. Predicting Young's modulus of nanowires from first-principle calculations on their surface and bulk materials. J. Appl. Phys. 104 (2009) 113517.

[39] F.J. Humphries, M. Hatherly. Recrystallization and Related Annealing Phenomena, Elsevier, Oxford, UK, 2005.

[40] D.J. Bacon, U/F. Kocks, R.O. Scattergood. The effect of dislocation self-interaction on the Orowan stress. Phil, Mag. 28 (1973) 1241-1263.